General sample size analysis for probabilities of causation: a delta method approach

Tianyuan Cheng[1], Ruirui Mao[2], Judea Pearl[3], and Ang Li[4]

[1]Department of Statistics, Florida State University
[2]Department of Computer Science, Cornell University
[3]Department of Computer Science, University of California Los Angeles
[4]Department of Computer Science, Florida State University

Abstract

Probabilities of causation (PoCs), such as the probability of necessity and sufficiency (PNS), are important tools for decision making but are generally not point identifiable. Existing work has derived bounds for these quantities using combinations of experimental and observational data. However, there is very limited research on sample size analysis, namely, how many experimental and observational samples are required to achieve a desired margin of error. In this paper, we propose a general sample size framework based on the delta method. Our approach applies to settings in which the target bounds of PoCs can be expressed as finite minima or maxima of linear combinations of experimental and observational probabilities. Through simulation studies, we demonstrate that the proposed sample size calculations lead to stable estimation of these bounds.

1 Introduction

Probabilities of causation (PoCs) are used in many real-world applications, such as marketing, law, social science, and health science, especially when decisions depend on whether an action caused an outcome. For example, Li and Pearl (2022) introduced a "benefit function" that is a linear combination of PoCs and reflects the payoff or cost of selecting an individual with certain features, with the goal of finding those most likely to show a target behavior. Robins and Greenland (1989) used PoCs for individual-level causal attribution in epidemiology and legal settings, where one asks how likely it is that an exposure caused an observed outcome for a specific case, and Stott et al. (2004) used it in climate event assignment to quantify how much human influence changes the risk of an extreme event. Mueller and Pearl (2023) argued that PoCs can be used for personalized decision making, and Li et al. (2020) found that PoCs can be helpful for improving the accuracy of some machine learning methods.

Without extra assumptions, PoCs are generally not identifiable, so one often works with bounds instead of point values. Using the structural causal model (SCM), Pearl (1999) defined three binary PoCs, including PNS, PN, and PS. Tian and Pearl (2000) derived bounds for these

quantities using both experimental and observational information, and later Li and Pearl (2019, 2024) provided formal proofs. Several papers studied how to tighten these bounds. For example, Mueller et al. (2021) used covariates and causal structure to narrow the bounds for PNS, and Dawid et al. (2017) used covariates to narrow the bounds for PN.

Most of these works implicitly assume that the experimental and observational samples are large enough to estimate the needed probabilities well. However, there is little work on how to choose sample sizes so that the estimated bounds have a desired level of precision. This gap limits the use of the theory in real applications. Li et al. (2022) discussed this issue, but focused on a special case for the PNS bound. To our knowledge, there is still no unified framework that links a target error level to required experimental and observational sample sizes for general PoC bounds.

In this paper, we study adequate sample sizes for estimating bounds of PoCs from a general perspective. Our starting point is that many sharp bounds can be written as a finite minimum or maximum of explicit functions of a finite set of probabilities, including experimental probabilities such as $P(y_x)$ and observational probabilities such as $P(x, y)$. For PNS, the bound components are typically linear in these probabilities; for PN and PS, the bound components often take a ratio form. Under mild regularity conditions (for example, denominators bounded away from zero), these bound components are smooth transformations of the underlying probability vector, which makes them suitable for multivariate delta-method analysis.

Our main contributions are:

- We propose a general sample size framework for estimating PoC bounds with a pre-specified margin of error, based on multivariate delta-method variance approximations.

- Our asymptotic results apply whenever the bound endpoints can be expressed as finite minima or maxima of explicit bound components. This covers common forms in the PoC literature and also extends to other bounded causal quantities, including linear combinations of PoCs.

- We provide simulation studies showing that the proposed sample sizes are stable and sufficient in practice, and that they are far less conservative than existing results in the literature.

2   Preliminaries

In this section, we briefly review the definitions of the three aspects of binary causation following Tian and Pearl (2000). Our analysis is based on the counterfactual framework within structural causal models (SCMs) as introduced in Pearl (2009). We denote by $Y_x = y$ the counterfactual statement that variable Y would take value y if X were set to x. Throughout the paper, we use y_x to represent the event $Y_x = y$, $y_{x'}$ for $Y_{x'} = y$, y'_x for $Y_x = y'$, and $y'_{x'}$ for $Y_{x'} = y'$. Experimental information is summarized through causal quantities such as $P(y_x)$, while observational information is summarized by joint distributions such as $P(x, y)$. Unless otherwise stated, X denotes the treatment variable and Y denotes the outcome variable.

For the following three probabilities of causation, we all assume that X and Y are two binary variables in a causal model M. Let x and y stand for the propositions $X = $ true and $Y = $ true, respectively, and x' and y' for their complements. Then we have:

Definition 1 (Probability of Necessity (PN))**.** The probability of necessity is defined as:

$$
\begin{aligned}
\text{PN} &\triangleq P(Y_{x'} = \text{false} \mid X = \text{true}, Y = \text{true}) \\
&\triangleq P(y'_{x'} \mid x, y).
\end{aligned}
\tag{1}
$$

Definition 2 (Probability of Sufficiency (PS))**.** The probability of sufficiency is defined as:

$$
\begin{aligned}
\text{PS} &\triangleq P(Y_x = \text{true} \mid X = \text{false}, Y = \text{false}) \\
&\triangleq P(y_x \mid x', y').
\end{aligned}
\tag{2}
$$

Definition 3 (Probability of Necessity and Sufficiency (PNS))**.** The probability of necessity and sufficiency is defined as:

$$
\begin{aligned}
\text{PNS} &\triangleq P(Y_x = \text{true}, Y_{x'} = \text{false}) \\
&\triangleq P(y_x, y'_{x'}).
\end{aligned}
\tag{3}
$$

We also introduce the sharp bounds on the PoCs derived from experimental and observational data in Tian and Pearl (2000), where the bounds are obtained via Balke's program in Balke (1995). The bounds are:

$$
\max \left\{ \begin{array}{l} 0, \\ P(y_x) - P(y_{x'}), \\ P(y) - P(y_{x'}), \\ P(y_x) - P(y) \end{array} \right\} \leq \text{PNS} \leq \min \left\{ \begin{array}{l} P(y_x), \\ P(y_{x'}), \\ P(x,y) + P(x',y'), \\ P(y_x) - P(y_{x'}) + P(x,y') + P(x',y) \end{array} \right\}.
\tag{4}
$$

$$
\max \left\{ 0, \frac{P(y) - P(y_{x'})}{P(x,y)} \right\} \leq \text{PN} \leq \min \left\{ 1, \frac{P(y'_{x'}) - P(x',y')}{P(x,y)} \right\}.
\tag{5}
$$

$$
\max \left\{ 0, \frac{P(y_x) - P(y)}{P(x',y')} \right\} \leq \text{PS} \leq \min \left\{ 1, \frac{P(y_x) - P(x,y)}{P(x',y')} \right\}.
\tag{6}
$$

3 Main Results

Let θ be a parameter vector that collects all experimental and observational probabilities we need. For example, in the setting of the upper bound of (4) we can take

$$
\theta = (P(y_x), P(y_{x'}), P(x,y), P(x',y'), P(x,y'), P(x',y))^\top.
\tag{7}
$$

We first claim that in most scenarios, the bounds of PoCs can be written in the form of a complex linear combination of θ.

Lemma 1 (Piecewise-linear and fractional forms of sharp bounds for PoCs)**.** Consider a structural causal model with finite discrete variables, and focus on the case that X and Y are both binary, *i.e.*, X has two treatment levels x, x' and Y has two outcome levels y, y'. Let $\theta \in \mathbb{R}^d$ collect the observational and experimental probabilities used to constrain the model.

For a probability of causation $Q \in \{\mathrm{PNS}, \mathrm{PN}, \mathrm{PS}\}$ as defined in Section 2, let $U_\mathrm{Q}(\theta)$ and $L_\mathrm{Q}(\theta)$ be its sharp upper and lower bounds over all SCMs. Then there exist finite positive integers $J, K < \infty$, vectors $a_j, c_k \in \mathbb{R}^d$ and constants $b_j, d_k \in \mathbb{R}$ such that

$$U_\mathrm{Q}(\theta) = \frac{1}{h_Q(\theta)} \min_{1 \leq j \leq J} \{a_j^\top \theta + b_j\}, \quad L_\mathrm{Q}(\theta) = \frac{1}{h_Q(\theta)} \max_{1 \leq k \leq K} \{c_k^\top \theta + d_k\}, \tag{8}$$

where the denominator $h_Q(\theta)$ is defined as:

1. For PNS: $h_{\mathrm{PNS}}(\theta) = 1$ (reducing to a piecewise-linear form).

2. For PN: $h_{\mathrm{PN}}(\theta) = P(x, y)$, which is a specific component of θ.

3. For PS: $h_{\mathrm{PS}}(\theta) = P(x', y')$, which is a specific component of θ.

$U_Q(\theta)$ and $L_Q(\theta)$ are continuous and piecewise-defined functions of θ. They are differentiable at any θ where the optimizer is unique.

Proof. According to Tian and Pearl (2000), for finite discrete SCMs, sharp bounds for PNS (and the numerators of PN, PS) can be obtained by optimizing a linear functional over the set of latent-type distributions consistent with θ, which is a linear programming (LP) problem. Then, by LP duality and the polyhedral structure of the dual feasible set (see Boyd and Vandenberghe (2004)), the optimal value is a piecewise-linear function of θ and has a finite min or max representation of linear functions $a^\top \theta + b$. $\qquad \square$

Lemma 1 gives a unified form for the sharp bounds: for PNS they are piecewise-linear in θ while for PN and PS they are piecewise linear-fractional due to normalization by $P(x, y)$ and $P(x', y')$. In either case, the bound endpoints are piecewise smooth and are differentiable whenever the active term is unique (optimizer is unique), and thus the inference for the plug-in estimators $\widehat{U_Q} = U_Q(\hat{\theta})$ and $\widehat{L_Q} = L_Q(\hat{\theta})$ reduces to studying piecewise-defined functions of $\hat{\theta}$. Next, we establish asymptotic normality and confidence intervals in the regular case where the optimizer is unique.

We first state the setup: let m be the experimental sample size and n be the observational sample size. Assume r is the ratio of experimental sample size to observational sample size, *i.e.*, $m/n \to r \in (0, \infty)$. Let $\theta = (\theta_e^\top, \theta_o^\top)^\top \in \mathbb{R}^d$ collect the experimental and observational probabilities used in Lemma 1, with true value $\theta_0 = (\theta_{e0}^\top, \theta_{o0}^\top)^\top \in \mathbb{R}^d$. Let $\hat{\theta} = (\hat{\theta}_e^\top, \hat{\theta}_o^\top)^\top$ be the plug-in estimator based on the two independent samples. By the multivariate central limit theorem (CLT) for multinomial proportions,

$$\sqrt{m} (\hat{\theta}_e - \theta_{e0}) \Rightarrow N(0, \Sigma_e), \qquad \sqrt{n} (\hat{\theta}_o - \theta_{o0}) \Rightarrow N(0, \Sigma_o), \tag{9}$$

and the two limits are independent. Equivalently,

$$\sqrt{n} (\hat{\theta} - \theta_0) \Rightarrow N(0, \Omega_r), \ \Omega_r = \begin{pmatrix} \Sigma_e/r & 0 \\ 0 & \Sigma_o \end{pmatrix}. \tag{10}$$

4

Theorem 1. Assume $h_Q(\theta_0) > 0$. Let

$$j^* = \arg\min_{1 \le j \le J}\{a_j^\top \theta_0 + b_j\}, \qquad k^* = \arg\max_{1 \le k \le K}\{c_k^\top \theta_0 + d_k\},$$

and assume both optimizers are unique with positive gaps:

$$\Delta_U := \min_{j \ne j^*}(a_j^\top \theta_0 + b_j) - (a_{j^*}^\top \theta_0 + b_{j^*}) > 0,$$

$$\Delta_L := (c_{k^*}^\top \theta_0 + d_{k^*}) - \max_{k \ne k^*}(c_k^\top \theta_0 + d_k) > 0.$$

Suppose $\sqrt{n}\,(\hat\theta - \theta_0) \Rightarrow N(0, \Omega_r)$. Then U_Q and L_Q are differentiable at θ_0 and

$$\begin{aligned}
\sqrt{n}\,(\hat{U}_Q - U_Q(\theta_0)) &\Rightarrow N\Big(0,\ \nabla U_Q(\theta_0)^\top \Omega_r\, \nabla U_Q(\theta_0)\Big), \\
\sqrt{n}\,(\hat{L}_Q - L_Q(\theta_0)) &\Rightarrow N\Big(0,\ \nabla L_Q(\theta_0)^\top \Omega_r\, \nabla L_Q(\theta_0)\Big).
\end{aligned} \tag{11}$$

$\square$

Proof. We prove the result for the upper bound U_Q only and the proof for lower bound is similar. Define

$$g(\theta) := \min_{1 \le j \le J}\{a_j^\top \theta + b_j\}, \qquad U_Q(\theta) = \frac{g(\theta)}{h_Q(\theta)}.$$

By assumption, the minimizer at θ_0 is unique and has a positive gap:

$$\Delta_U = \min_{j \ne j^*}\big(a_j^\top \theta_0 + b_j\big) - \big(a_{j^*}^\top \theta_0 + b_{j^*}\big) > 0.$$

Since each $a_j^\top \theta + b_j$ is continuous and the index set is finite, the gap implies that there exist a $\epsilon > 0$ such that for all $\|\theta - \theta_0\| \le \epsilon$, the minimizer is j^*. Hence $g(\theta)$ is differentiable at θ_0. By Danskin's theorem (Danskin (2012)),

$$\nabla g(\theta_0) = a_{j^*}.$$

Because h_Q is differentiable at θ_0 and $h_Q(\theta_0) > 0$, it yields that U_Q is differentiable at θ_0 with

$$\nabla U_Q(\theta_0) = \frac{h_Q(\theta_0)\nabla g(\theta_0) - g(\theta_0)\nabla h_Q(\theta_0)}{h_Q(\theta_0)^2} = \frac{h_Q(\theta_0)a_{j^*} - (a_{j^*}^\top \theta_0 + b_{j^*})\nabla h_Q(\theta_0)}{h_Q(\theta_0)^2}.$$

Now apply the multivariate delta method to the differentiable map $\theta \mapsto U_Q(\theta)$ at θ_0:

$$\sqrt{n}\big(U_Q(\hat\theta) - U_Q(\theta_0)\big) \Rightarrow N\Big(0,\ \nabla U_Q(\theta_0)^\top \Omega_\tau\, \nabla U_Q(\theta_0)\Big). \tag{12}$$

$\square$

Using Theorem 1 we can derive a corresponding confidence interval as follows:

5

Corollary 1. Assume the conditions of Theorem 1. Let $\widehat{\Omega}_r$ be a consistent estimator of Ω_r. Define the plug-in variance estimators

$$\widehat{V}_U := \nabla U_Q(\widehat{\theta})^\top \widehat{\Omega}_r \nabla U_Q(\widehat{\theta}), \qquad \widehat{V}_L := \nabla L_Q(\widehat{\theta})^\top \widehat{\Omega}_r \nabla L_Q(\widehat{\theta}),$$

and the corresponding standard errors

$$\widehat{\mathrm{SE}}(\widehat{U}_Q) := \sqrt{\widehat{V}_U/n}, \qquad \widehat{\mathrm{SE}}(\widehat{L}_Q) := \sqrt{\widehat{V}_L/n}.$$

Then, asymptotic $(1 - \alpha)$ confidence intervals for $U_Q(\theta_0)$ and $L_Q(\theta_0)$ are

$$\widehat{U}_Q \pm z_{1-\alpha/2}\,\widehat{\mathrm{SE}}(\widehat{U}_Q), \qquad \widehat{L}_Q \pm z_{1-\alpha/2}\,\widehat{\mathrm{SE}}(\widehat{L}_Q), \tag{13}$$

where $z_{1-\alpha/2}$ can be found on z-table of standard normal distribution. □

Proof. By Theorem 1, we have

$$\sqrt{n}\big(\widehat{U}_Q - U_Q(\theta_0)\big) \Rightarrow N(0, V_U), \qquad V_U := \nabla U_Q(\theta_0)^\top \Omega_r \nabla U_Q(\theta_0),$$

and similarly

$$\sqrt{n}\big(\widehat{L}_Q - L_Q(\theta_0)\big) \Rightarrow N(0, V_L), \qquad V_L := \nabla L_Q(\theta_0)^\top \Omega_r \nabla L_Q(\theta_0).$$

Let $\widehat{\Omega}_r$ be a consistent estimator of Ω_r. Under the uniqueness conditions in Theorem 1, U_Q and L_Q are differentiable in a neighborhood of θ_0, hence $\nabla U_Q(\cdot)$ and $\nabla L_Q(\cdot)$ are continuous at θ_0. Since $\widehat{\theta} \xrightarrow{p} \theta_0$, we have

$$\nabla U_Q(\widehat{\theta}) \xrightarrow{p} \nabla U_Q(\theta_0), \qquad \nabla L_Q(\widehat{\theta}) \xrightarrow{p} \nabla L_Q(\theta_0).$$

Therefore, by Slutsky's theorem (Van der Vaart (2000)),

$$\widehat{V}_U := \nabla U_Q(\widehat{\theta})^\top \widehat{\Omega}_r \nabla U_Q(\widehat{\theta}) \xrightarrow{p} V_U, \qquad \widehat{V}_L := \nabla L_Q(\widehat{\theta})^\top \widehat{\Omega}_r \nabla L_Q(\widehat{\theta}) \xrightarrow{p} V_L.$$

Define $\widehat{\mathrm{SE}}(\widehat{U}_Q) = \sqrt{\widehat{V}_U/n}$ and $\widehat{\mathrm{SE}}(\widehat{L}_Q) = \sqrt{\widehat{V}_L/n}$. Then

$$\frac{\widehat{U}_Q - U_Q(\theta_0)}{\widehat{\mathrm{SE}}(\widehat{U}_Q)} \Rightarrow N(0,1), \qquad \frac{\widehat{L}_Q - L_Q(\theta_0)}{\widehat{\mathrm{SE}}(\widehat{L}_Q)} \Rightarrow N(0,1), \tag{14}$$

which gives an asymptotic $(1 - \alpha)$ confidence intervals. □

When the unique-optimizer assumption in Theorem 1 fails, means that when we have multiple active constraints, then the bound function may be non-differentiable at θ_0. In this case we use a directional delta method (see Dümbgen (1993), Fang and Santos (2019)) to derive the limiting distribution. The following theorem states the result.

Theorem 2. Let $U_Q(\theta)$ and $L_Q(\theta)$ be defined as in equation (8). Assume $h_Q(\theta_0) > 0$ and h_Q is differentiable at θ_0. Define the active sets as follows:

$$J_0 = \arg \min_j (\, a_j^\top \theta_0 + b_j), \qquad K_0 = \arg \max_k (c_k^\top \theta_0 + d_k).$$

If $\sqrt{n}(\hat{\theta} - \theta_0) \Rightarrow Z \sim N(0, \Omega_r)$, then

$$\sqrt{n}(\widehat{U}_Q - U_Q(\theta_0)) \Rightarrow \min_{j \in J_0} g_{U,j}^\top Z, \qquad \sqrt{n}(\widehat{L}_Q - L_Q(\theta_0)) \Rightarrow \max_{k \in K_0} g_{L,k}^\top Z,$$

where the generalized gradients at θ_0 are

$$g_{U,j} = \frac{a_j}{h_Q(\theta_0)} - \frac{\min_\ell (a_\ell^\top \theta_0 + b_\ell)}{h_Q(\theta_0)^2} \nabla h_Q(\theta_0), \qquad j \in J_0.$$

$$g_{L,k} = \frac{c_k}{h_Q(\theta_0)} - \frac{\max_\ell (c_\ell^\top \theta_0 + d_\ell)}{h_Q(\theta_0)^2} \nabla h_Q(\theta_0), \qquad k \in K_0.$$

$\square$

In general, the limiting distribution in Theorem 2 is not Gaussian. Instead, it is the distribution of a minimum or maximum of finitely many correlated Gaussian linear forms evaluated at the Gaussian limit $Z \sim N(0, \Omega_r)$. To obtain the corresponding confidence interval we can simulate Z and compute directional-derivative functionals as shown in Theorem 2.

Remark 1. The representation in Lemma 1 is not specific to PoCs. The same form holds for any causal quantity whose sharp bounds can be written as in the form of equation (8) with $h(\theta) > 0$ and finite J, K. All asymptotic results in Theorems 1 continue to hold under the same setup and assumptions.

4 Simulation

In this section we run experiments to show that the proposed number of samples provided by Theorems and Corollary in last section are adequate to obtain PoCs within the desired margin errors. We study the bounds for PNS, which is one of the most frequently used PoCs in causal studies. For comparison, we use the same simulation setup as Li et al. (2022), which studies the sharp PNS bound given in Section 2. It is trivial to verify that this sharp bound has the form shown in Lemma 1.

4.1 Experiment: estimating PNS bound

Following Li et al. (2022), we consider two parameter settings that share the same causal graph in Figure 1 but differ in their coefficients. Here X is a binary treatment with $x = 1$, $x' = 0$, Y is a binary outcome with $y = 1$, $y' = 0$, and $Z = (Z_1, \ldots, Z_{20})$ is a set of 20 mutually independent binary covariates. Detailed coefficients are provided in Supplementary materials.
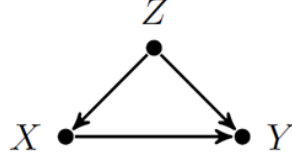
Figure 1: The Causal model for PNS bound experiment. X and Y are binary, and Z is a set of 20 independent binary confounders.

Let U_{Z_i}, U_X, and U_Y be independent Bernoulli exogenous variables. The endogenous covariates are defined as follows:

$$Z_i = U_{Z_i}, \qquad i = 1, \ldots, 20,$$

and

$$M_X = \sum_{i=1}^{20} a_i Z_i, \qquad M_Y = \sum_{i=1}^{20} b_i Z_i,$$

where $\{a_i\}$ and $\{b_i\}$ are drawn from Uniform$(-1, 1)$. Here are the structural equations and we generate (X, Y) following these equations with a constant $C \sim$ Uniform$(-1, 1)$:

$$X = f_X(M_X, U_X) = \begin{cases} 1, & \text{if } M_X + U_X > 0.5, \\ 0, & \text{otherwise,} \end{cases}$$

$$Y = f_Y(X, M_Y, U_Y) = \begin{cases} 1, & 0 < CX + M_Y + U_Y < 1, \text{ or } 1 < CX + M_Y + U_Y < 2, \\ 0, & \text{otherwise.} \end{cases}$$

Since all exogenous variables are binary and independent, the population experimental quantities (e.g., $P(y_x)$ and $P(y_{x'})$) and the population observational quantities (e.g., $P(x, y')$ and $P(x', y)$) can be computed exactly by summing over all configurations of $(U_X, U_Y, U_{Z_1}, \ldots, U_{Z_{20}})$. For instance, we can compute

$$P(y_x) = \sum_{u_X, u_Y, \mathbf{u}_Z} P(u_X) P(u_Y) \prod_{i=1}^{20} P(u_{Z_i}) f_Y\big(1, M_Y(\mathbf{u}_Z), u_Y\big),$$

and

$$P(x, y) = \sum_{u_X, u_Y, \mathbf{u}_Z} P(u_X) P(u_Y) \prod_{i=1}^{20} \Big[P(u_{Z_i}) \cdot f_X\big(M_X(\mathbf{u}_Z), u_X\big) \cdot f_Y\big(f_X, M_Y(\mathbf{u}_Z), u_Y\big) \Big],$$

where $\mathbf{u}_Z = (u_{Z_1}, \ldots, u_{Z_{20}})$ and $M_X(\mathbf{u}_Z), M_Y(\mathbf{u}_Z)$ denote the corresponding realizations of M_X and M_Y.

We then generate finite samples under two rules. For the experimental sample of size m, we draw $(U_X, U_Y, U_{Z_1}, \ldots, U_{Z_{20}})$ from their Bernoulli distributions, assign $X \sim$ Bernoulli(0.5)

8

independently of the exogenous variables, and set $Y = f_Y(X, M_Y, U_Y)$. This will give i.i.d. experimental pairs (X, Y). Let m_{ab} be the number of experimental samples with $(X = a, Y = b)$ and $m_{a\cdot} = m_{a0} + m_{a1}$. We estimate

$$\widehat{P}(y_x) = \widehat{P}(Y = 1 \mid X = 1) = \frac{m_{11}}{m_{1\cdot}}, \qquad \widehat{P}(y_{x'}) = \widehat{P}(Y = 1 \mid X = 0) = \frac{m_{01}}{m_{0\cdot}}.$$

For the observational sample of size n, we again draw the exogenous variables, set $X = f_X(M_X, U_X)$ and $Y = f_Y(X, M_Y, U_Y)$, and estimate the required joint probabilities by empirical frequencies. Let n_{ab} be the number of observational samples with $(X = a, Y = b)$ and $n = \sum_{a \in \{0,1\}} \sum_{b \in \{0,1\}} n_{ab}$. For example,

$$\widehat{P}(x, y) = \frac{n_{11}}{n}, \quad \widehat{P}(x, y') = \frac{n_{10}}{n}, \quad \widehat{P}(x', y) = \frac{n_{01}}{n}.$$

These estimated probabilities are then plugged into the bound formulas to get finite-sample bound estimates.

Assume the ratio of experimental data to observational data is $m/n \to r = 1$. Then, Corollary 1 gives adequate experimental size $m \geq 1921$, while result provided in Li et al. (2022) gives $m \geq 6147$. Our method requires only about 31% of the sample size suggested by the existing result. The detailed computation is in Supplementary material.
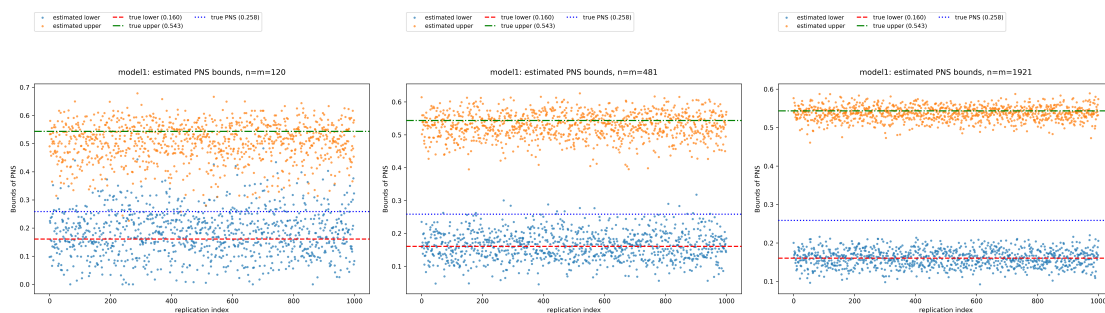

Figure 2: Scatter plots under different sample sizes for Model 1. Left to right: $n = 120, 481, 1921$.

For both Model 1 and 2, we run 1000 replications, and in each replication, we generate experimental and observational samples with sizes $n \in \{120, 481, 1921\}$. The results are shown in Figures 2 and 3. When $n = 120$, both bounds are highly noisy with large dispersion across replications. Increasing the sample size to $n = 481$ reduces the noise, but the variance remains relatively large. When $n = 1921$, the adequate size we computed using Theorem 1, we can see that the estimates become very stable, with both the upper and lower bound concentrates tightly around the true bounds, which shows a good accuracy and stability.

We also examine the relationship between sample size n and the average estimation error, defined as $\widehat{(\mathrm{bound} - \mathrm{true\ bound})}$ averaged over 1000 replications for each model. See Figure 4. Using the target error level 0.05(red horizontal line), both Model 1 and Model 2 reach the desired accuracy with sample sizes below 300 for both the upper and lower bounds (blue/orange
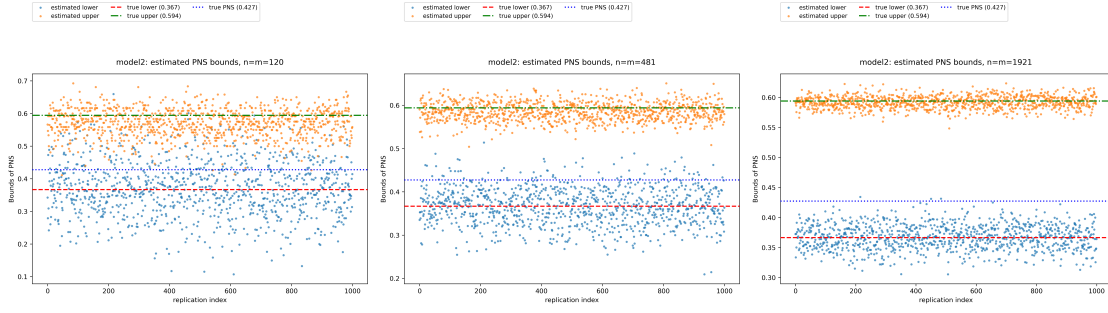
9

Figure 3: Scatter plots under different sample sizes for Model 2. Top to bottom: $n = 120, 481, 1921$.

curves). The average error drops quickly as n increases up to around 500, which suggests that $n = 500$ can already work well in practice. This also confirms that the theoretical sample size $n = 1921$ is more than sufficient and it represents the adequate size that considers the worst case.
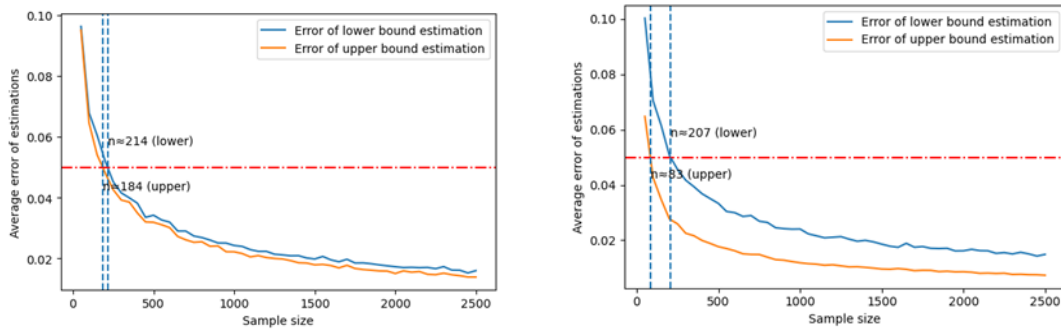

Figure 4: Average error of estimations VS sample size. Left: Model 1, Right:Model 2

We further investigate the relationship between the average estimation error and the sample size n beyond Models 1 and 2. In order to approximate a more general setting, we repeatedly resample the SCM coefficients and rerun the same simulation design as in Model 1 for 20 independent draws. For each n, we then average the estimation error over both the 1000 Monte Carlo replications, and report the resulting curve in Figure 5. It shows that both the upper and lower bound estimation errors decrease rapidly as n increases, and in this aggregated experiment the errors converge even faster than in Models 1 and 2. The target error level 0.05 is reached around 100, smaller than 500, which is consistent with our earlier observations. The theoretical sample size $n = 1921$ remains clearly sufficient with very small errors for both bounds. In summary, these results suggest that the sample-size selection rule using our Theorems is not tied to a single parameter setting and remains stable and accurate across a range of SCM with different coefficients.
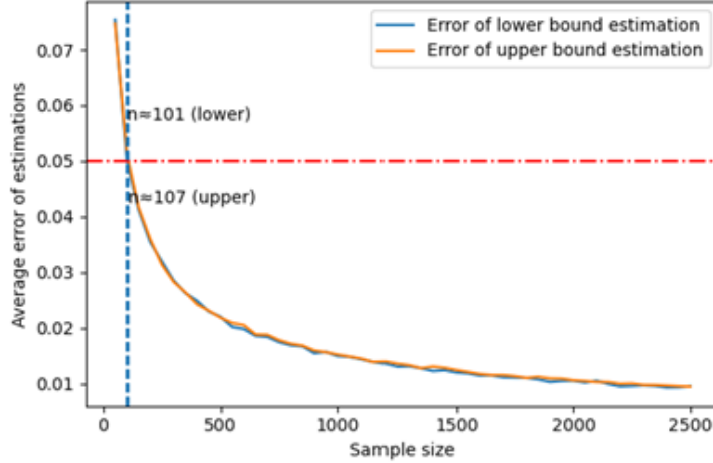
10

Figure 5: Average error with sample size for 20 replicates

5 Discussion

The bounds of PoCs are piecewise-defined, and points with multiple optimizers lie on the boundaries between pieces. Away from these boundaries, the optimizer is unique and thus Theorem 1 applies. Since the measure of boundary points are almost zero, we can think Theorem 1 holds for most of time. This is supported by our simulations, where the target error is often achieved with far fewer samples than the theoretical results (around $1/4$ to $1/3$), suggesting that the active piece is quite stable in a neighborhood of θ_0.

For the non-unique optimizer case in Theorem 2, one may consider a smooth approximation (*e.g.*, Softmin) to enforce differentiability, but this introduces approximation bias and requires hyperparameter tuning. For this reason we adopt a conservative variance-based approach. However, smoothing may still be useful for large-scale repeated evaluations or gradient-based optimization when near-ties are common and numerical stability is a concern.

Most importantly, although we use PoCs (PNS, PN, PS) in binary setup as motivating examples, Theorems 1 and 2 apply more broadly. We discuss two extensions here. First, our proposed method can be directly extended to multi-level discrete X and Y, with the same CLT and (directional) delta-method arguments but at the cost of higher dimension and computational difficulty. Second, the same methods can be applied to any bounded causal quantity whose sharp bounds can be written as a finite minimum or maximum of linear (or ratio-type) functions of θ, including linear combinations of PoCs such as the "benefit function" in Li and Pearl (2019).

6 Conclusion

We study the adequate sample size for estimating bounds of PoCs within a desired margin of error. In finite discrete settings, we first show that the bounds can be written as finite minima or maxima of explicit functions of observational and experimental probabilities, including

11

both linear and ratio-type terms. Using this representation, we propose a general sample size framework based on multivariate delta-method variance approximations. Our asymptotic results apply whenever the bound endpoints has this finite min max form, which covers many bounds in related literature and also extends to other bounded causal quantities, including linear combinations of PoCs. We also provide simulation studies showing that the proposed sample sizes are stable and work well in practice, and are less conservative than existing approaches. To our knowledge, this is the first work that offers a general and systematic framework for analyzing adequate sample sizes for estimating non-identifiable PoCs.

References

Balke, A. A. (1995). *Probabilistic counterfactuals: semantics, computation, and applications*. University of California, Los Angeles.

Boyd, S. and Vandenberghe, L. (2004). *Convex optimization*. Cambridge university press.

Danskin, J. M. (2012). *The theory of max-min and its application to weapons allocation problems*, volume 5. Springer Science & Business Media.

Dawid, A. P., Musio, M., and Murtas, R. (2017). The probability of causation. *Law, Probability and Risk*, 16(4):163–179.

Dümbgen, L. (1993). On nondifferentiable functions and the bootstrap. *Probability Theory and Related Fields*, 95(1):125–140.

Fang, Z. and Santos, A. (2019). Inference on directionally differentiable functions. *The Review of Economic Studies*, 86(1):377–412.

Li, A., J. Chen, S., Qin, J., and Qin, Z. (2020). Training machine learning models with causal logic. In *Companion Proceedings of the Web Conference 2020*, pages 557–561.

Li, A., Mao, R., and Pearl, J. (2022). Probabilities of causation: Adequate size of experimental and observational samples. *arXiv preprint arXiv:2210.05027*.

Li, A. and Pearl, J. (2019). Unit selection based on counterfactual logic. In *Proceedings of the Twenty-Eighth International Joint Conference on Artificial Intelligence*.

Li, A. and Pearl, J. (2022). Unit selection with causal diagram. In *Proceedings of the AAAI conference on artificial intelligence*, volume 36, pages 5765–5772.

Li, A. and Pearl, J. (2024). Probabilities of causation with nonbinary treatment and effect. In *Proceedings of the AAAI conference on artificial intelligence*, volume 38, pages 20465–20472.

Mueller, S., Li, A., and Pearl, J. (2021). Causes of effects: Learning individual responses from population data. *arXiv preprint arXiv:2104.13730*.

Mueller, S. and Pearl, J. (2023). Personalized decision making–a conceptual introduction. *Journal of Causal Inference*, 11(1):20220050.

Pearl, J. (1999). Probabilities of causation: Three counterfactual interpretations and their identification. *Synthese*, 121(1-2):93.

Pearl, J. (2009). *Causality*. Cambridge university press.

Robins, J. and Greenland, S. (1989). The probability of causation under a stochastic model for individual risk. *Biometrics*, pages 1125–1138.

Stott, P. A., Stone, D. A., and Allen, M. R. (2004). Human contribution to the european heatwave of 2003. *Nature*, 432(7017):610–614.

Tian, J. and Pearl, J. (2000). Probabilities of causation: Bounds and identification. *Annals of Mathematics and Artificial Intelligence*, 28(1):287–313.

Van der Vaart, A. W. (2000). *Asymptotic statistics*, volume 3. Cambridge university press.